The Journal of Neuroscience, September 1, 1999, *19*(17):7495–7506

Mitochondrial Clearance of Cytosolic Ca^{2+} in Stimulated Lizard Motor Nerve Terminals Proceeds without Progressive Elevation of Mitochondrial Matrix [Ca^{2+}]

Gavriel David

Department of Physiology and Biophysics, University of Miami School of Medicine, Miami Florida 33101

This study used fluorescent indicator dyes to measure changes in cytosolic and mitochondrial [Ca^{2+}] produced by physiological stimulation of lizard motor nerve terminals. During repetitive action potential discharge at 10–50 Hz, the increase in average cytosolic [Ca^{2+}] reached plateau at levels that increased with increasing stimulus frequency. This stabilization of cytosolic [Ca^{2+}] was caused mainly by mitochondrial Ca^{2+} uptake, because drugs that depolarize mitochondria greatly increased the stimulation-induced elevation of cytosolic [Ca^{2+}], whereas blockers of other Ca^{2+} clearance routes had little effect. Surprisingly, during this sustained Ca^{2+} uptake the free [Ca^{2+}] in the mitochondrial matrix never exceeded a plateau level of ~1 μM, regardless of stimulation frequency or pattern. When stimulation ceased, matrix [Ca^{2+}] decreased over a slow (~10 min) time course consisting of an initial plateau followed by a return to baseline. These measurements demonstrate that sustained mitochondrial Ca^{2+} uptake is not invariably accompanied by progressive elevation of matrix free [Ca^{2+}]. Both the plateau of matrix free [Ca^{2+}] during stimulation and its complex decay after stimulation could be accounted for by a model incorporating reversible formation of an insoluble Ca salt. This mechanism allows mitochondria to sequester large amounts of Ca^{2+} while maintaining matrix free [Ca^{2+}] at levels sufficient to activate Ca^{2+}-dependent mitochondrial dehydrogenases, but below levels that activate the permeability transition pore.

Key words: mitochondria; mitochondrial calcium uptake; presynaptic terminal; motor nerve terminal; mitochondrial matrix; calcium indicator dyes; calcium buffering; calcium sequestration

Isolated mitochondria take up Ca^{2+} via a uniporter in the inner mitochondrial membrane (for review, see Gunter and Pfeiffer, 1990). Application of drugs that depolarize mitochondria has demonstrated that mitochondrial Ca^{2+} uptake is important for buffering/sequestering moderate-to-large Ca^{2+} loads in neuronal somata, axons, presynaptic terminals, and secretory cells (Alnaes and Rahamimoff, 1975; Baker and Schlaepfer, 1978; Åkerman and Nicholls, 1981; Martínez-Serrano and Satrústegui, 1992; Stuenkel, 1994; Friel and Tsien, 1994; Werth and Thayer, 1994; White and Reynolds, 1995; Herrington et al., 1996; Park et al., 1996; Sidky and Baimbridge, 1997). In support of this idea, fluorescent Ca^{2+} indicator dyes in the mitochondrial matrix report an increase in free [Ca^{2+}] in depolarized bovine adrenal chromaffin cells (Babcock et al., 1997). In lizard motor nerve terminals, mitochondrial Ca^{2+} uptake contributes importantly to limiting the increase in average cytosolic [Ca^{2+}] during brief stimulus trains (David et al., 1998).

The present study used this motor terminal preparation to study how mitochondria influence nerve terminal Ca^{2+} metabolism during and after longer stimulus trains. If mitochondrial Ca^{2+} uptake is limited, occurring only during initial phases of stimulation, then other plasma membrane/endoplasmic reticular Ca^{2+} extrusion/sequestration mechanisms would be expected to contribute importantly to Ca^{2+} handling during longer stimulus trains. If instead mitochondria continue to take up Ca^{2+} during prolonged stimulus trains, then Ca^{2+} in the mitochondrial matrix would have to be buffered or otherwise sequestered to prevent dissipation of the gradient permitting passive Ca^{2+} entry. Indeed, the bound/free ratio estimated for calcium in matrix is ~3000–4000, compared with ~100 estimated in cytosol (Babcock et al. 1997; Magnus and Keizer, 1997). If matrix Ca^{2+} is buffered primarily by conventional buffers, one would expect matrix free [Ca^{2+}] to continue to rise throughout stimulation.

Mitochondria can also contain precipitated Ca salts. Electron microscopic studies have documented the formation of electron-dense structures, including granules, within the matrix of mitochondria exposed to large Ca^{2+} loads (LeFurgey et al., 1988), including mitochondria within nerve terminals subjected to intense stimulation (Párducz and Jóo, 1976; Jóo et al., 1980). An important question is whether such salt formation contributes to buffering of matrix Ca^{2+} (for review, see Nicholls and Åkerman, 1982) or occurs only when mitochondria are exposed to pathologically high Ca^{2+} loads and/or certain fixation procedures (Somlyo et al., 1979) (for review, see Brown et al., 1985; Carafoli, 1987). If such salt formation occurs in stimulated nerve terminals, one would expect matrix free [Ca^{2+}] to rise at first but then reach plateau at a level near the salt's solubility product.

This study tested these hypotheses by measuring changes in cytosolic and matrix free [Ca^{2+}] in lizard motor nerve terminals stimulated under physiological conditions. I demonstrate that matrix free [Ca^{2+}] increases early during a stimulus train but then stops increasing after ~100 action potentials, at a level that is relatively independent of stimulation frequency. Pharmacological evidence indicates that mitochondrial Ca^{2+} uptake continues, although matrix free [Ca^{2+}] stops increasing. When stimu-

Received May 17, 1999; revised June 21, 1999; accepted June 23, 1999.

This work was supported by National Institutes of Health Grant RO1 NS 12404. I thank Drs. Ellen Barrett and John Barrett for help with this manuscript and valuable discussions, Ying Wang and Dr. Glenn Kerrick for measuring the Ca^{2+} affinity of Oregon green BAPTA-5N, and Dr. Anna Suter (Ciba-Geigy Pharmaceuticals) for providing CGP 37157.

Correspondence should be addressed to Dr. Gavriel David, Department of Physiology and Biophysics, R-430, University of Miami School of Medicine, P.O. Box 016430, Miami FL 33101.

lation stops, matrix free [Ca^{2+}] exhibits a prolonged plateau followed by a decay to baseline over a time course of minutes. The pattern of changes in cytosolic and mitochondrial free [Ca^{2+}] during and after a stimulus train can be accounted for by a model that includes reversible precipitation of a Ca salt in the mitochondrial matrix.

MATERIALS AND METHODS

Preparation. External intercostal neuromuscular preparations were dissected from lizards (*Anolis sagrei*) that were killed by pithing and decapitation after ether anesthesia. Preparations were mounted and viewed as described in David et al. (1998). The physiological saline contained (in mM): 157 NaCl, 4 KCl, 2 $CaCl_2$, 2 $MgCl_2$, and 1 HEPES. The motor nerve was stimulated by applying brief, suprathreshold depolarizing pulses (0.1–0.2 msec) via a suction electrode. Muscle contractions were usually blocked by adding carbachol (150–200 μM) or D-tubocurare (10 mg/l) to the bath. Experiments were performed at room temperature (20–25°C). In a few experiments (see Fig. 1*B*), end-plate potentials were monitored via a KCl-filled microelectrode inserted into the muscle fiber in the end-plate region [as in David et al. (1997)].

In some experiments (as noted in the figure legends), the visibility of the imaged terminal was improved by crushing the ends of the underlying muscle fiber with a sharp glass micropipette in saline containing trypsin (1 mg/ml, washed out 2–4 min after crushing the muscle). In some muscle fibers this treatment clarified the cytoplasm in the end-plate region, improving the visibility of motor nerve terminals synapsing on them (see Fig. 2*A*) and ensuring that fluorescence from mitochondria in the end-plate region of the muscle fiber (David et al., 1998) did not affect the measurements of mitochondrial [Ca^{2+}] in nerve terminals. Stimulation-induced changes in cytosolic and mitochondrial [Ca^{2+}] in trypsin-treated terminals were similar to those measured in preparations with intact muscle fibers.

Fluorometric measurement of cytosolic and mitochondrial [Ca^{2+}]. Changes in cytosolic [Ca^{2+}] were monitored using Oregon green-BAPTA 5N (OG-5N) loaded ionophoretically as the K salt via a microelectrode inserted into the motor axon (David et al., 1997). This form of OG-5N is membrane-impermeable and hence does not enter organelles.

Changes in mitochondrial [Ca^{2+}] were monitored in terminals bath-loaded with the membrane-permeable acetoxymethylester (AM) forms of dihydrorhod-2, rhod-2, or OG-5N [5–10 μg/ml for 2–3 hr, prepared from 1000× stock solutions in dimethylsulfoxide (DMSO)]. Preparations were then washed with indicator-free medium for ≥3 hr before the onset of imaging. Dihydrorhod-2 fluoresces only after it is oxidized to rhod-2, which occurs preferentially within mitochondria (Hajnóczky et al., 1995). The AM forms of fluorescent indicator dyes can cross not only the plasma membrane but also the membranes surrounding intracellular compartments such as mitochondria, and the AM moiety can be cleaved by esterases in both cytosol and intracellular compartments. In this preparation, dyes loaded from the bath in their AM form using the protocol described above tended to localize within mitochondria, as judged by four criteria. First, fluorescence was clustered in the terminal rather than distributed continuously throughout the cytosol of the terminal and axon (Fig. 2, compare photographs in *A*, *B*). Second, after the onset of stimulation the increase in fluorescence began with a delay, in contrast to the immediate increase measured with dyes injected ionophoretically into the cytosol. [This differential delay is not evident on the time scales shown here but was evident with the faster sampling used in David et al. (1998).] Third, after stimulation ceased, fluorescence decayed with a very slow time course relative to the initial fast decay of cytosolic [Ca^{2+}] (Fig. 2, compare *A*, *B*). Fourth, the stimulation-induced increase in fluorescence was blocked by agents that depolarize mitochondria [carbonyl cyanide m-chlorophenylhydrazone (CCCP), antimycin A1, rotenone; see Fig. 2*A*] but not by agents that release Ca^{2+} from endoplasmic reticulum (ER) (Fig. 4*B*).

A likely reason why AM-loaded dyes compartmentalized within organelles is that during the ≥3 hr washout period, dye in the terminal cytosol was diluted by diffusion into the axon. (The perineurial and myelin sheaths prevented axonal uptake of dye from the bath.) Thus the only dye remaining in the terminal was that contained within relatively nonmobile intracellular compartments. We cannot exclude the possibility that dye trapped within the ER made some contribution to the resting fluorescence, but the pharmacological manipulations mentioned above indicated that the main compartment exhibiting stimulation-induced changes in fluorescence was that of the mitochondria, which are abundant in these motor terminals (Walrond and Reese, 1985). Dye localization in this preparation therefore depended strongly on the loading technique, with ionophoretic injection of the salt filling primarily the cytosol, and bath-loading of the AM form filling primarily organelles such as mitochondria.

In experiments like that in Figure 1 involving simultaneous measurement of mitochondrial and cytosolic [Ca^{2+}], mitochondrial rhod-2 and cytosolic OG-5N were excited with 488 nm light, and a dichroic mirror was used to separate the emitted light into a red component from rhod-2 (>570 nm) and a green component from OG-5N (535 ± 20 nm). Measurements were corrected for "cross-talk" between rhod-2 and OG-5N signals as described in David et al. (1998).

Rhod-2 binds Ca^{2+} with a K_d of ~0.5 μM. The K_d of OG-5N is much higher: ~60 μM (see below). Thus changes in OG-5N fluorescence were approximately linearly related to changes in cytosolic and mitochondrial [Ca^{2+}]. The exact concentration of dyes in the cytosol and mitochondrial matrix could not be measured, but OG-5N has such a low affinity that it was unlikely to buffer a significant amount of Ca^{2+} in cytosol or matrix. Also, fluorescence transients recorded in mitochondria filled with the high-affinity rhod-2 had time courses similar to those recorded in mitochondria filled with OG-5N. Thus the presence of dyes as exogenous buffers did not seriously distort the phenomena under study.

Fluorescence was monitored using a confocal laser-scanning microscope (Odyssey XL, Noran Instruments, Middleton, WI). Images were collected (≥0.266 sec/image) using an Indy workstation (Silicon Graphics) with Noran InterVision software, and stored and analyzed as described in David et al. (1997). The number of images collected in a given experiment was limited by the available computer memory and by the need to limit overall laser exposure to avoid tissue damage. Thus images were collected either frequently for a short period, or infrequently over longer periods. Fluorescence was plotted in one of two ways: (1) as $\Delta F/F_{rest}$ (abbreviated as $\Delta F/F$), where ΔF is the change in fluorescence and F_{rest} is resting (prestimulation) fluorescence, or (2) as net fluorescence (after subtraction of background), to assess the slow decay of mitochondrial [Ca^{2+}] and effects of drugs on resting [Ca^{2+}]. Fluorescence was averaged over regions of interest that included all dye-labeled terminal regions. In dual-imaging studies the regions of interest defined for OG-5N were also used to analyze rhod-2 fluorescence.

OG-5N fluorescence changes were converted into estimates of [Ca^{2+}] changes as described in David et al. (1997), using the following equation: $[Ca^{2+}] = K_d[(\Delta F/F_{rest} + 1 - 1/\beta)/(F_{max}/F_{rest} - \Delta F/F_{rest} - 1)]$, where $\beta = F_{rest}/F_{min} = (K_d + ([Ca^{2+}]_{rest})(F_{max}/F_{min}))/(K_d + [Ca^{2+}]_{rest})$.

The K_d for OG-5N was 50–70 μM, and the ratio F_{max}/F_{min} ranged from 20 to 30 in *in vitro* measurements made over the pH range 6.5–7.5 (Ying Wang and Dr. W. Glenn L. Kerrick, personal communication). Calculations assumed a resting free [Ca^{2+}] of 100 nM for both cytosol and mitochondria (for review, see Babcock and Hille, 1998).

Preparations were checked for stability by administering the same stimulus train several times at 15 min intervals. Under control conditions, $\Delta F/F$ transients were quite stable (Figs. 1*C*, 2*C*), displaying little evidence of the "rundown" often observed in internally dialyzed cells. Terminals exhibiting abrupt increases in F_{rest} were not analyzed further.

Changes in mitochondrial membrane potential were monitored using 5,5′,6,6′-tetrachloro-1,1′,3,3′-tetra-ethylbenzimidazolylcarbocyanine iodide (JC-1), 20 min exposure to 5 μg/ml, followed by wash (DiLisa et al., 1995). The excitation wavelength was 488 nm; an increase in the ratio of green (<570 nm) to red (>570 nm) emissions indicates depolarization.

Reagents. Indicator dyes were purchased from Molecular Probes (Eugene, OR). CGP 37157 was the kind gift of Dr. Anna Suter of Ciba-Geigy Pharmaceuticals (Basel, Switzerland). Ru360 was from Calbiochem (San Diego, CA). All other reagents were from Sigma (St. Louis, MO). Antimycin A1 and oligomycin were added from 1000× stock solutions in DMSO and ethanol, respectively. Cyclopiazonic acid (CPA) was added from 50 mM stock in DMSO, thapsigargin from 10 mM stock in DMSO, and caffeine was dissolved fresh in H_2O. Digitonin solution was prepared from 10 mM stock in DMSO.

RESULTS

Mitochondrial free [Ca^{2+}] attains a plateau during prolonged stimulation

Figure 1*A* plots stimulation-induced $\Delta F/F$ transients measured in a motor nerve terminal containing OG-5N in the cytosol and

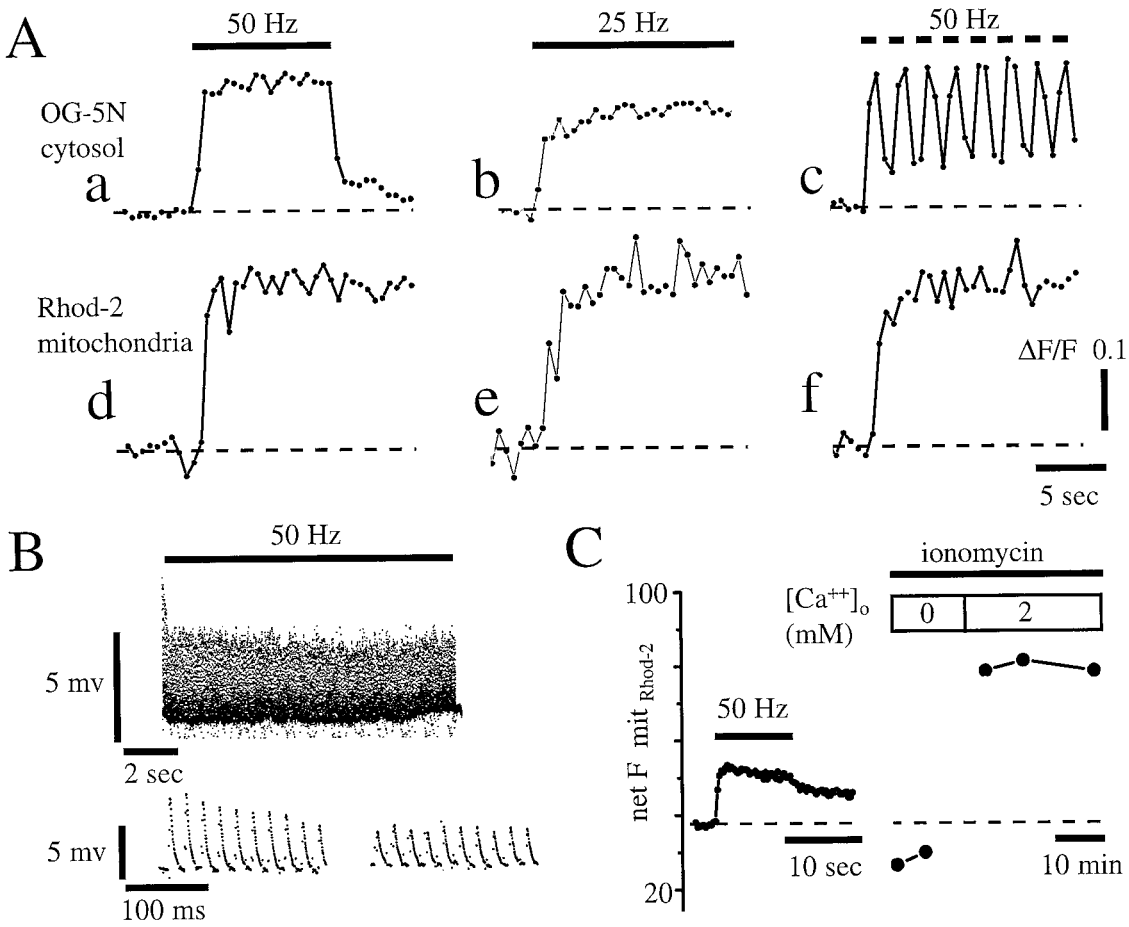

Figure 1. Changes in fluorescence of Ca^{2+} indicator dyes in cytosol and mitochondria and end-plate potentials (EPPs) during repetitive stimulation of motor nerve terminals. *A*, $\Delta F/F$ for cytosolic OG-5N (*a–c*) and mitochondrial rhod-2 (*d–f*) recorded simultaneously during stimulation at 50 Hz (*a*, *d*) and 25 Hz (*b*, *e*), and with an intermittent pattern (*c*, *f*; 1 sec at 50 Hz alternating with 1 sec rest; 0.533 sec/image). *Top horizontal bars* indicate duration of stimulation. *B*, EPPs recorded from a different end-plate during a 50 Hz, 10 sec stimulus train like that in *A*, *a*. *Top trace* shows all EPPs on a slow time scale; *bottom trace* shows first 10 (*left*) and last 10 (*right*) EPPs sampled on a faster time scale. The ends of the muscle fiber were cut to depolarize the resting potential to approximately −40 mV; this procedure minimized contractions, enabling recordings at normal quantal content without use of nicotinic antagonists. *C*, Changes in net fluorescence of mitochondrial rhod-2 (*net F mit*$_{Rhod\text{-}2}$) in a different terminal. *Left record* shows two superimposed 50 Hz, 10 sec trains separated by a 10 min rest. *Right record* shows fluorescence in the presence of 5 μM ionomycin, first in saline containing no added Ca^{2+} and 2 mM BAPTA, then in normal 2 mM Ca^{2+} saline. Note the different time scales for the stimulation and ionomycin data. In this preparation the cytoplasm of the underlying muscle fiber was cleared by cutting muscle fiber ends in trypsin, as described in Materials and Methods.

rhod-2 in mitochondria (see Materials and Methods). The terminal was stimulated with a 50 Hz train lasting 10 sec, with a prolonged 25 Hz train, and with an alternating pattern (50 Hz for 1 sec followed by 1 sec rest). During sustained stimulation at 50 and 25 Hz, both cytosolic and mitochondrial [Ca^{2+}] increased rapidly at first but later stabilized at a plateau level. The amplitude of the cytosolic plateau was greater during 50 Hz than during 25 Hz stimulation [as also reported by Ravin et al. (1997); David et al. (1998); Ohnuma et al. (1999)], but the amplitude of the mitochondrial plateau was similar for both stimulation frequencies. During the intermittent stimulation pattern, cytosolic [Ca^{2+}] fell rapidly during rest periods, but mitochondrial [Ca^{2+}] did not. Rather, the amplitude of the mitochondrial fluorescence transient was similar for both steady and intermittent patterns of stimulation. The finding that the initial decay of mitochondrial [Ca^{2+}] was much slower than that for cytosolic [Ca^{2+}] agrees with the findings of Babcock et al. (1997) after depolarizing pulses in adrenal chromaffin cells.

Figure 1*B* shows that end-plate potentials continued to be evoked in the underlying muscle fiber throughout prolonged stimulus trains. Because evoked transmitter release requires Ca^{2+} entry through depolarization-activated Ca^{2+} channels, this result demonstrates that the failure of cytosolic and mitochondrial free [Ca^{2+}] to continue rising during maintained stimulation was not caused by cessation of Ca^{2+} entry across the plasma membrane.

The plateau of mitochondrial [Ca^{2+}] during stimulation is not an artifact of dye saturation

The high Ca^{2+} affinity of rhod-2 raises the possibility that the plateau of its fluorescence during prolonged stimulation might have been caused by dye saturation. Figure 1*C* presents evidence that this was not the case: the maximal fluorescence of mitochondrial rhod-2 during 50 Hz stimulation was less than that measured when the terminal was subsequently exposed to ionomycin (a Ca^{2+} ionophore) in the presence of 2 mM bath Ca^{2+}.

To test further whether the fluorescence increase of mitochondrial indicator dyes was limited by dye saturation, mitochondria were instead AM-loaded with the lower-affinity OG-5N, whose fluorescence is unlikely to saturate at any [Ca^{2+}] achieved within

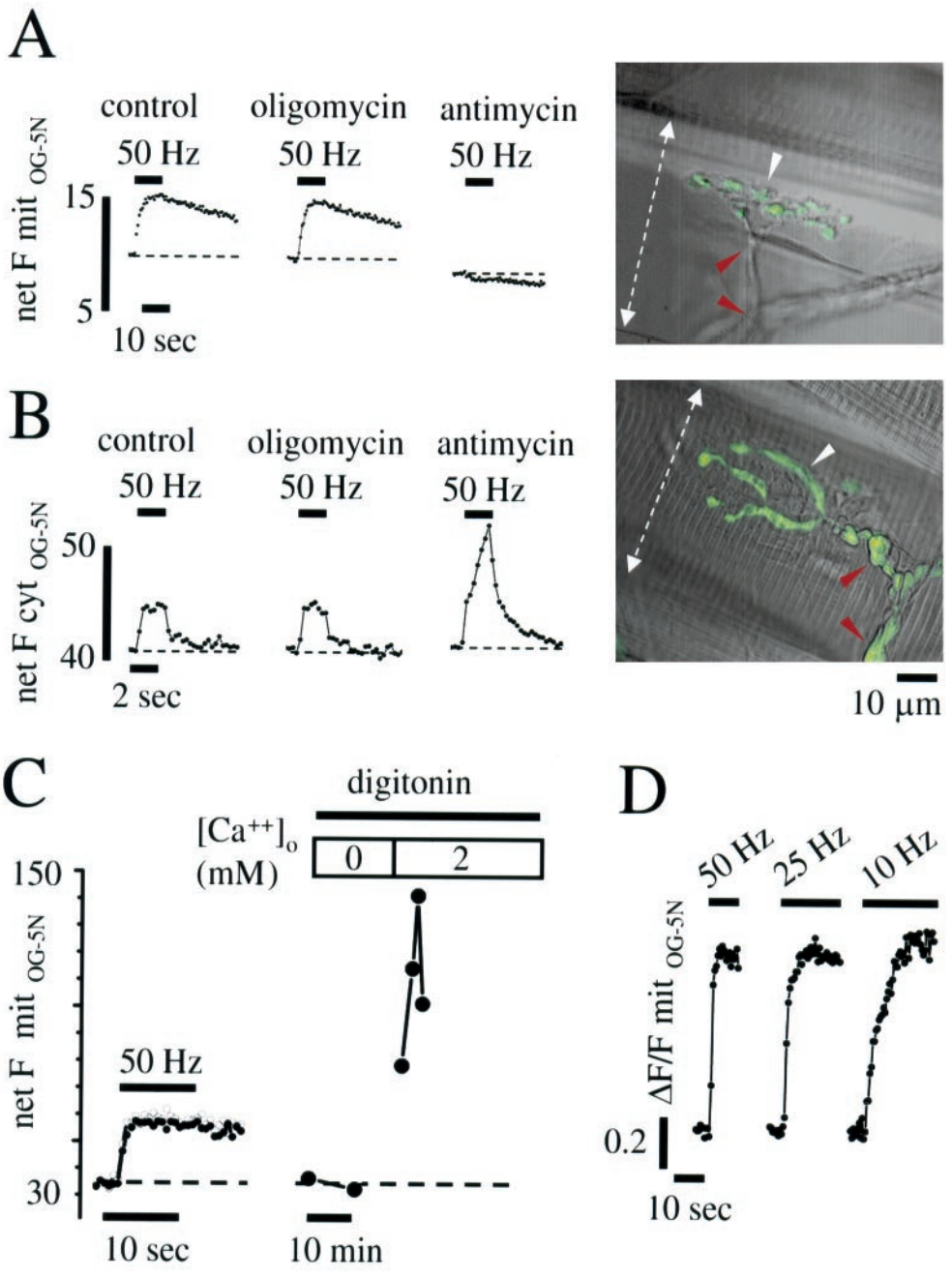

Figure 2. Stimulation-induced fluorescence transients recorded with OG-5N loaded into mitochondria or cytosol. *A*, *B*, OG-5N net fluorescence in mitochondria (*A*) and cytosol (*B*) during 50 Hz stimulation in control saline, 15 min after application of oligomycin (5 μg/ml) and 5 min after addition of antimycin A1 (2 μM). Photographs show OG-5N fluorescence (*green*) superimposed on transmitted-light images (*white arrowhead* indicates motor terminal; *red arrowheads* indicate axon; *arrows* connected by *dotted lines* indicate muscle fiber in *B*, and "ghost" of cleared muscle fiber in *A*). In *A*, 2 mM phosphate was present in all solutions. *C*, Changes in net fluorescence of mitochondrial OG-5N in a different terminal. *Left records* show superimposed responses to two 50 Hz, 10 sec trains. *Right records* show response to changes in bath [Ca^{2+}] when membranes were permeabilized with digitonin (5 μM). The preparation in digitonin was initially washed with an intracellular-like saline containing 150 mM K-gluconate, 2 mM Na-pyruvate, 2 mM Na-lactate, and 2 mM BAPTA, and then washed with a similar saline containing 2 mM Ca^{2+} and no BAPTA. The large increase in net fluorescence after Ca^{2+} addition was followed by loss of fluorescence, probably caused by loss of dye from mitochondria (digitonin-induced permeabilization of mitochondrial inner membrane and/or opening of the mitochondrial permeability transition pore). *D*, Δ*F*/*F* for mitochondrial OG-5N in a different terminal stimulated at 50 Hz for 10 sec, 25 Hz for 20 sec, and 10 Hz for 25 sec. Trains were separated by 20 min rest intervals. Muscle fibers were cleared in *A*, *C*, and *D*. Imaging at 0.533 sec/image in *A*, *C*, *D*; 0.266 sec/image in *B*.

living cells (Fig. 2*A*). The OG-5N Δ*F*/*F* transients in Figure 2*A* confirm its mitochondrial localization: the stimulation-induced fluorescence increase declined slowly (rather than rapidly) after stimulation and was blocked by antimycin A1, which collapses the membrane potential across the inner mitochondrial membrane by irreversibly inhibiting complex III in the electron transport chain.

In contrast, when OG-5N was injected ionophoretically into the axonal cytosol, its fluorescence was visible within the axon as well as the terminal (Fig. 2*B*). The stimulation-induced Δ*F*/*F* transient was *increased* by antimycin A1 and showed an initial steep decline when stimulation stopped (as in Fig. 1*A*, *a*,*c*). Rotenone (5 μM), which inhibits electron transport at complex I, produced effects similar to those of antimycin A1 (data not shown). Oligomycin, which inhibits ATP synthase but does not depolarize mitochondria, had no effect on either cytosolic or mitochondrial Δ*F*/*F* transients (Fig. 2*A*,*B*), indicating that the changes produced by antimycin A1 and rotenone were caused by mitochondrial depolarization rather than inhibition of mitochondrial ATP synthesis.

Figure 2*C* shows that the fluorescence of OG-5N in mitochondria did not saturate during repetitive stimulation, because a larger fluorescence increase was measured when terminals were exposed to 2 mM bath Ca^{2+} in the presence of the detergent digitonin. Similar results were seen in another terminal permeabilized with ionomycin. Thus results in Figures 1*D* and 2*C*, combined with the fact that the plateau of mitochondrial fluorescence during prolonged stimulation was measured with low- as well as high-affinity dyes, suggest that this plateau was caused by stabilization of free [Ca^{2+}] in the matrix rather than saturation of the indicator dyes.

A possible concern about the experiments with ionomycin and

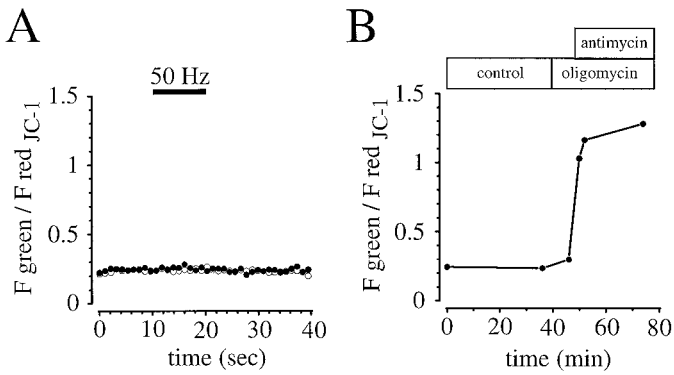

Figure 3. Effect of stimulation (*A*) and antimycin A1 (*B*) on mitochondrial membrane potential in a motor terminal, measured using JC-1. *A*, *Open* and *filled circles* show that stimulation (two 50 Hz, 10 sec trains) produced no detectable depolarization. *B*, Antimycin A1 (2 μM) depolarized mitochondria, but oligomycin alone (5 μg/ml) did not. Note the different time scales in *A* and *B*. The stimulus trains in *A* were delivered during the interval labeled *control* in *B*. Each point in *B* is the *green/red* JC-1 emissions ratio averaged from 40 images collected at 0.533 sec/image over a period of 21.3 sec.

digitonin is that some of the increase in fluorescence measured in AM-loaded preparations with 2 mM bath Ca^{2+} might have come from dye in ER, but any contribution from dye in the ER was probably negligible, because application of agents that deplete ER Ca^{2+} produced no change in resting fluorescence. Also, other conditions that would have been expected to cause ER Ca^{2+} to rise, e.g., stimulation in the presence of mitochondrial inhibitors, did not increase the fluorescence of AM-loaded dyes (Fig. 2*A*).

Mitochondrial free [Ca^{2+}] plateaus at ~1 μM during repetitive stimulation

Figure 2*D* shows mitochondrial OG-5N $\Delta F/F$ transients recorded during repetitive stimulation at 50, 25, and 10 Hz. The rate of rise of mitochondrial [Ca^{2+}] increased as stimulation frequency increased, but the final steady level was similar for all three frequencies (see also mitochondrial rhod-2 transients in Fig. 1*A*, *d–f*).

During 50 Hz stimulation, the maximal $\Delta F/F$ for cytosolic OG-5N averaged 0.20 ± 0.06 (SD, $n = 18$ terminals), whereas that for mitochondrial OG-5N averaged 0.43 ± 0.20 ($n = 12$). Assuming that OG-5N in cytosol and matrix has properties similar to those measured *in vitro*, these $\Delta F/F$ values suggest an increase in cytosolic [Ca^{2+}] within the range 0.35–0.74 μM and an increase in matrix [Ca^{2+}] within the range 0.75–1.62 μM (see Materials and Methods). The latter estimate might be too low if some of the resting fluorescence of AM-loaded dyes originates from intracellular compartments other than mitochondria.

Repetitive nerve stimulation produces no detectable mitochondrial depolarization

Figure 3 shows measurements of the emissions ratio of JC-1, an index of mitochondrial depolarization, during 50 Hz, 10 sec stimulus trains (Fig. 3*A*) and after application of oligomycin and antimycin A1 (Fig. 3*B*). The stimulus train, similar to that applied in Figures 1*A* and 2*A*, produced no detectable depolarization. The mitochondrial membrane potential was also maintained in oligomycin but depolarized when antimycin A1 was added (Fig. 3*B*).

The plateau of mitochondrial [Ca^{2+}] is not caused by accelerated activity of non-mitochondrial Ca^{2+} sequestration/extrusion mechanisms

One possible explanation for the finding that both cytosolic and mitochondrial [Ca^{2+}] attain steady states (rather than continuing to increase) during prolonged stimulation is a "relay race" hypothesis in which the Ca^{2+} that enters stimulated terminals is sequestered first by cytosolic buffers, second by mitochondrial uptake, and subsequently by other transport mechanisms in the ER and/or plasma membrane. Figure 4*A* shows that the magnitude of the stimulation-induced increase in mitochondrial [Ca^{2+}] was not altered when the plasma membrane Na^+/Ca^{2+} exchanger was inhibited by substituting Li^+ for Na^+ in the bathing solution. Figure 4*B*,*C* shows that CPA (20 μM), an inhibitor of ER Ca^{2+}-ATPase, did not alter the magnitude of mitochondrial or cytosolic [Ca^{2+}] transients, respectively. Caffeine (10 mM) (Fig. 4*B*), ryanodine, and thapsigargin (each at 10 μM; data not shown), which deplete certain ER Ca^{2+} stores, also produced no detectable change. CPA, caffeine, and ryanodine produced muscle contractures; the illustrated records were taken after these contractures subsided. Figure 4*D* shows that inhibition of plasma membrane Ca^{2+}-ATPase activity with alkaline pH (Milanick, 1990) was similarly without effect on the magnitude of cytosolic [Ca^{2+}] transients. These treatments to inhibit ER Ca^{2+} sequestration and plasma membrane Ca^{2+} extrusion also had little effect on resting cytosolic or mitochondrial [Ca^{2+}] over the time course studied here (data not shown).

In contrast, after addition of CCCP (1 μM), a protonophore that depolarizes mitochondria and thus inhibits mitochondrial Ca^{2+} uptake, cytosolic [Ca^{2+}] continued to increase throughout the stimulus train (Fig. 4*C*,*D*). These results, as well as those in Figure 2*A*,*B*, suggest that mitochondria continue to play a dominant role in limiting the increase in cytosolic [Ca^{2+}] during prolonged stimulation, even after the mitochondrial free [Ca^{2+}] reported by intramitochondrial dyes has stopped increasing.

I also tried to test for continued mitochondrial Ca^{2+} uptake using Ru360, reported to block selectively the mitochondrial Ca^{2+} uniporter in heart cells (Matlib et al., 1998). In motor nerve terminals, however, Ru360 (10–100 μM) produced a reversible, concentration-dependent reduction in stimulation-induced cytosolic [Ca^{2+}] transients (data not shown), suggesting that Ru360 reduced Ca^{2+} entry via plasma membrane Ca^{2+} channels (N-type) (David et al., 1997). Thus the effects of Ru360 were not specific for the uniporter in this preparation.

If during sustained stimulation mitochondria stabilize matrix free [Ca^{2+}] by increasing extrusion of Ca^{2+} via the mitochondrial Na^+/Ca^{2+} exchanger, inhibition of this exchanger with CGP 37157 (Cox and Matlib, 1993) would be expected to reduce the cytosolic [Ca^{2+}] measured during stimulation. Figure 5*A* shows that CGP 37157 did not have this effect but did reduce a slowly decaying component of the post-stimulation cytosolic [Ca^{2+}] transient thought to reflect Ca^{2+} extrusion from mitochondria, as also reported by Babcock et al. (1997). Cyclosporin A, which inhibits the mitochondrial permeability transition pore, another possible route of mitochondrial Ca^{2+} extrusion, had no effect on cytosolic [Ca^{2+}] transients during or after sustained stimulation (data not shown). These results thus suggest that the plateau of mitochondrial [Ca^{2+}] during prolonged stimulation is not caused by enhanced mitochondrial Ca^{2+} extrusion into the cytosol.

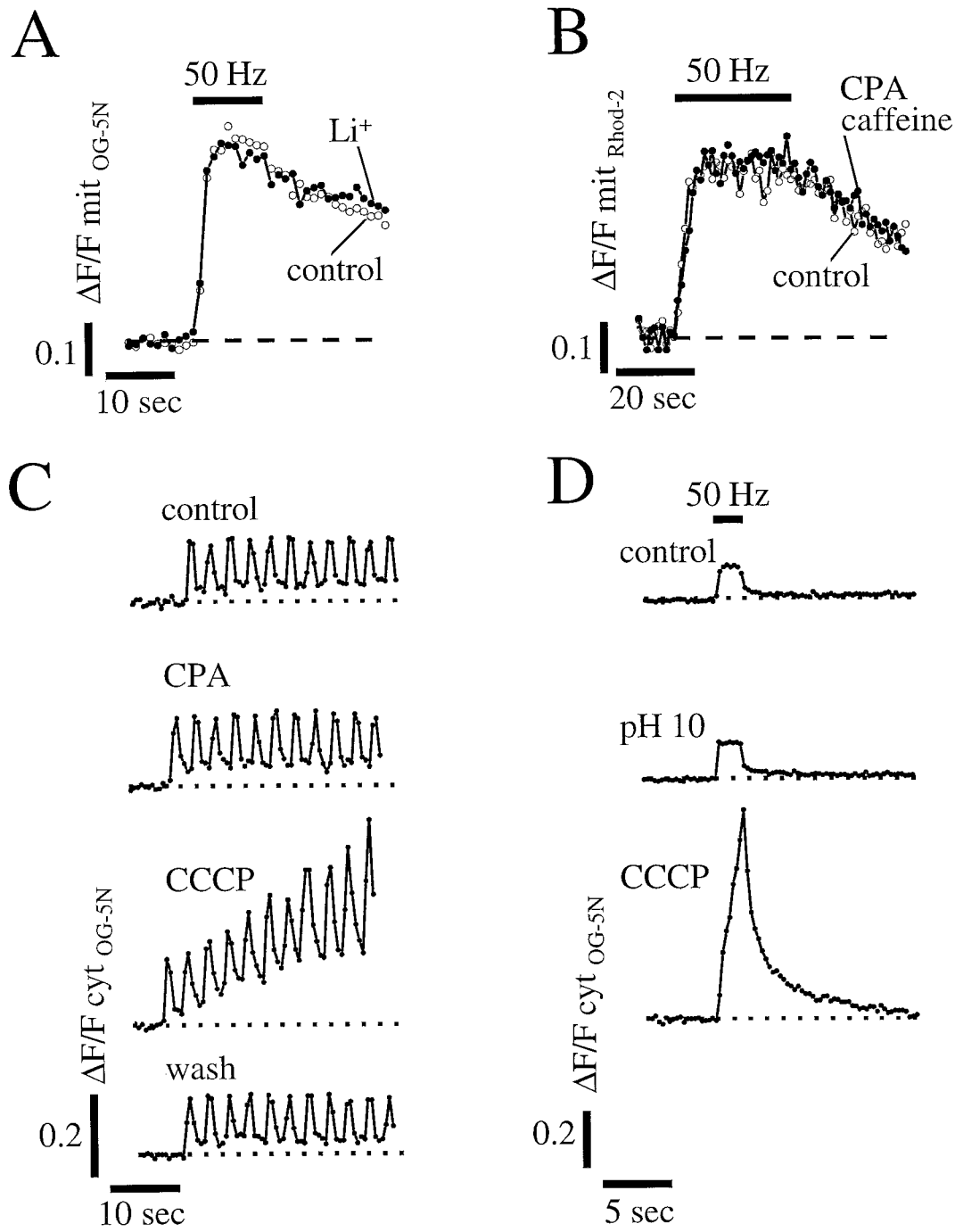

Figure 4. Effect of blocking various Ca^{2+} transport mechanisms on stimulation-induced $\Delta F/F$ transients. *A*, Superimposed mitochondrial OG-5N transients produced by 50 Hz stimulation in control saline (○) and 15 min after equimolar substitution of Li^+ for Na^+ (●) to block the plasma membrane Na^+/Ca^{2+} exchanger. (Li^+ passes through voltage-gated Na^+ channels and thus supports action potential propagation.) *B*, Superimposed mitochondrial rhod-2 transients produced by 50 Hz stimulation in control saline (○) and after addition of cyclopiazonic acid (*CPA*, 20 μM, 120 min) and caffeine (10 mM, 50 min) to deplete endoplasmic reticular Ca^{2+} stores (●). *C*, Cytosolic OG-5N transients produced by intermittent stimulation (50 Hz for 1 sec alternating with 2 sec rest) in control saline, 33 min after application of CPA (25 μM), 1 min after addition of CCCP (1 μM) to depolarize mitochondria, and 20 min after washout of both drugs. *D*, Cytosolic OG-5N transients produced by 50 Hz stimulation for 2 sec in control saline, 30 min after changing bath pH to 10 to inhibit the plasma membrane Ca^{2+} ATPase, and 9 min after application of CCCP (1 μM). In *A–D*, successive stimulation periods were separated by ≥15 min rest periods. Imaging is at 1.066 sec/image in *A* and *B*, 0.533 sec/image in *C*, and 0.266 sec/image in *D*. The muscle in *A* was cleared.

Some of the Ca stored in mitochondria is readily releasable

The above results suggest that during prolonged stimulation matrix free [Ca^{2+}] stabilizes, although mitochondria continue to take up Ca^{2+}. Such a result might occur if a Ca salt precipitates within the mitochondrial matrix. If so, one might wonder how readily the Ca within such a precipitate could be released. Figure 5*B* shows that application of CCCP after a brief stimulus train (100 stimuli at 50 Hz) produced no detectable elevation of cytosolic [Ca^{2+}], but that a similar CCCP application after a longer

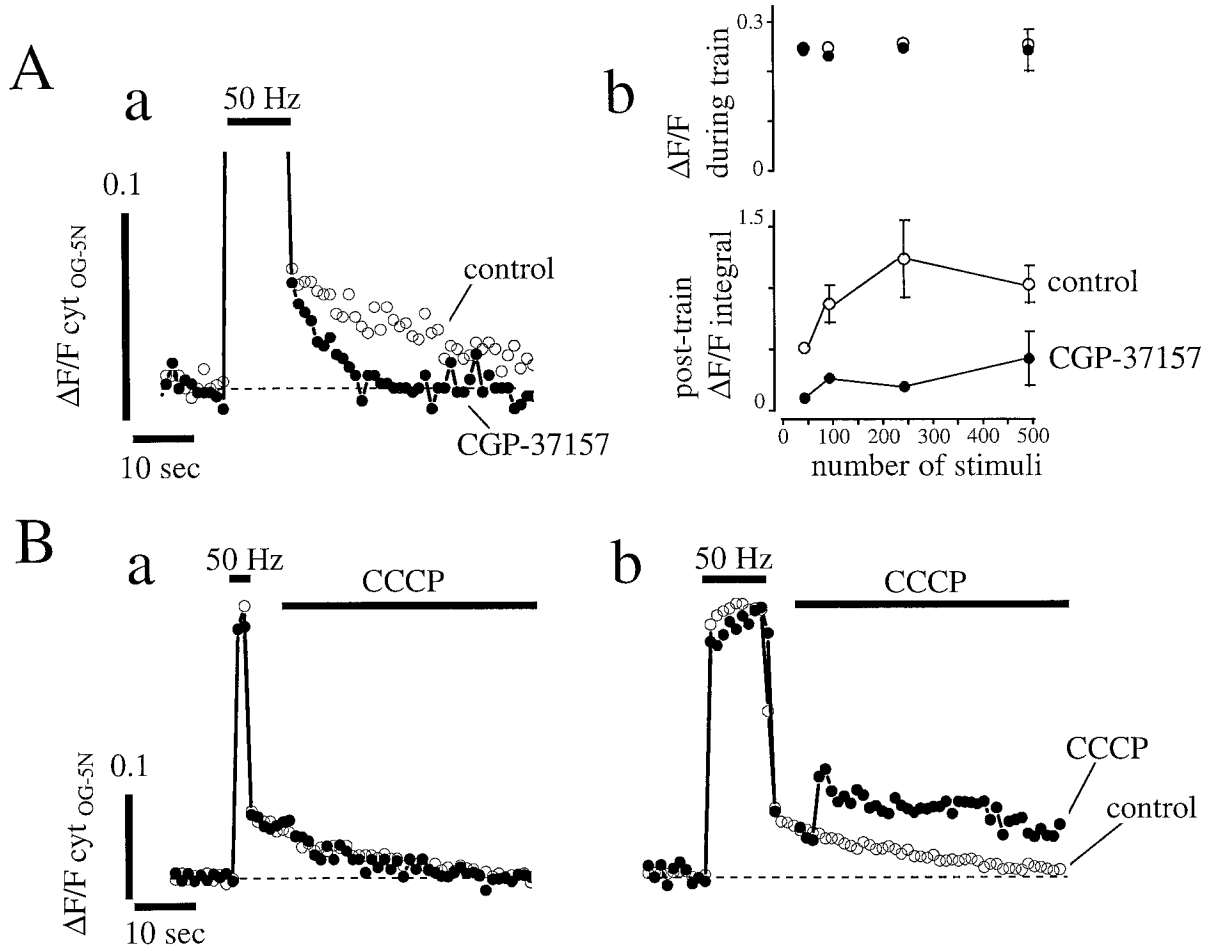

Figure 5. Effects of CGP 37157 (*A*) and post-train application of CCCP (*B*) on cytosolic OG-5N $\Delta F/F$ transients. *A*, *a*, Superimposed responses to 50 Hz, 10 sec trains before and ≥20 min after addition of CGP 37157 (●; 50 μM, prepared from 10 mM stock in DMSO). Each trace is an average of four repetitions separated by 15 min rest periods. *A*, *b*, *Top graph* plots average steady-state $\Delta F/F$ during the train as a function of train duration. *Bottom graph* plots post-train time integral of $\Delta F/F$, measured starting at the inflection point separating fast and slow decay phases on a semilogarithmic plot and ending 50 sec after cessation of stimulation (n = 2–4 for control trains, 4 for 500 stimuli CGP train, and 1 for all other CGP trains; error bars indicate ±2 SEM). *B*, *Superimposed traces* plot $\Delta F/F$ produced in another terminal by applying CCCP (2 μM; ●) after 50 Hz trains lasting 2 sec (*B*, *a*), or 10 sec (*B*, *b*). CCCP was applied over the interval indicated by the *top horizontal bars*, using a fast perfusion system that exchanged the solution in the experimental chamber. Imaging at 1.066 images/sec in both *A* and *B*.

train (500 stimuli) did elevate cytosolic [Ca^{2+}]. However, the elevation of cytosolic [Ca^{2+}] produced by post-train CCCP was small in comparison with the severalfold increase in cytosolic [Ca^{2+}] recorded when CCCP was applied *before* the stimulus train (Fig. 4*C*,*D*). The smaller post-train elevation of cytosolic [Ca^{2+}] suggests that elevating cytosolic Ca^{2+} via efflux from mitochondria is slower than elevating cytosolic Ca^{2+} via depolarization-activated Ca^{2+} channels in the plasma membrane. A more quantitative assessment of the effect of train duration on CCCP-evoked $\Delta F/F$ transients was not possible because of the muscle contractions often evoked by CCCP application and the long intertrain intervals required to reverse CCCP effects.

Mitochondrial [Ca^{2+}] decays with a slow and complex time course after stimulation

Figure 6*A* shows that the elevation of mitochondrial [Ca^{2+}] produced by a train of 500 stimuli decayed with a complex time course lasting ~10 min. Immediately after the train, mitochondrial [Ca^{2+}] decayed very slowly, followed by a more rapid phase of decay to baseline (see also Fig. 6*C*). The prolonged and complex time course of decay was not caused by light damage or dye bleaching induced by repeated laser scanning, because a similarly prolonged decay was evident when imaging was minimized during the decay (Fig. 6*B*). Also, post-train decays were similar (within experimental error) before and after an interval without imaging (Fig. 6*C*). The slow decay was not caused by the intramitochondrial dye acting as an exogenous buffer, because the same slow decay was seen in mitochondria filled with the low-affinity dye OG-5N (data not shown), which would be expected to bind less Ca^{2+} than the higher affinity rhod-2. This slow release of mitochondrial Ca^{2+} contributes a slow component to the decay of cytosolic [Ca^{2+}] and hence to short-term synaptic memory (Tang and Zucker, 1997). It is unclear whether matrix [Ca^{2+}] ever falls as low *in vivo* as the baseline values measured here, because intercostal motor nerve terminals in a breathing animal might never experience 15 min periods of inactivity.

Another interesting feature of the fluorescence transients shown in Figure 6*B*,*C* is that the increment in mitochondrial free [Ca^{2+}] produced by a 50 Hz train (1–10 sec) was larger when a

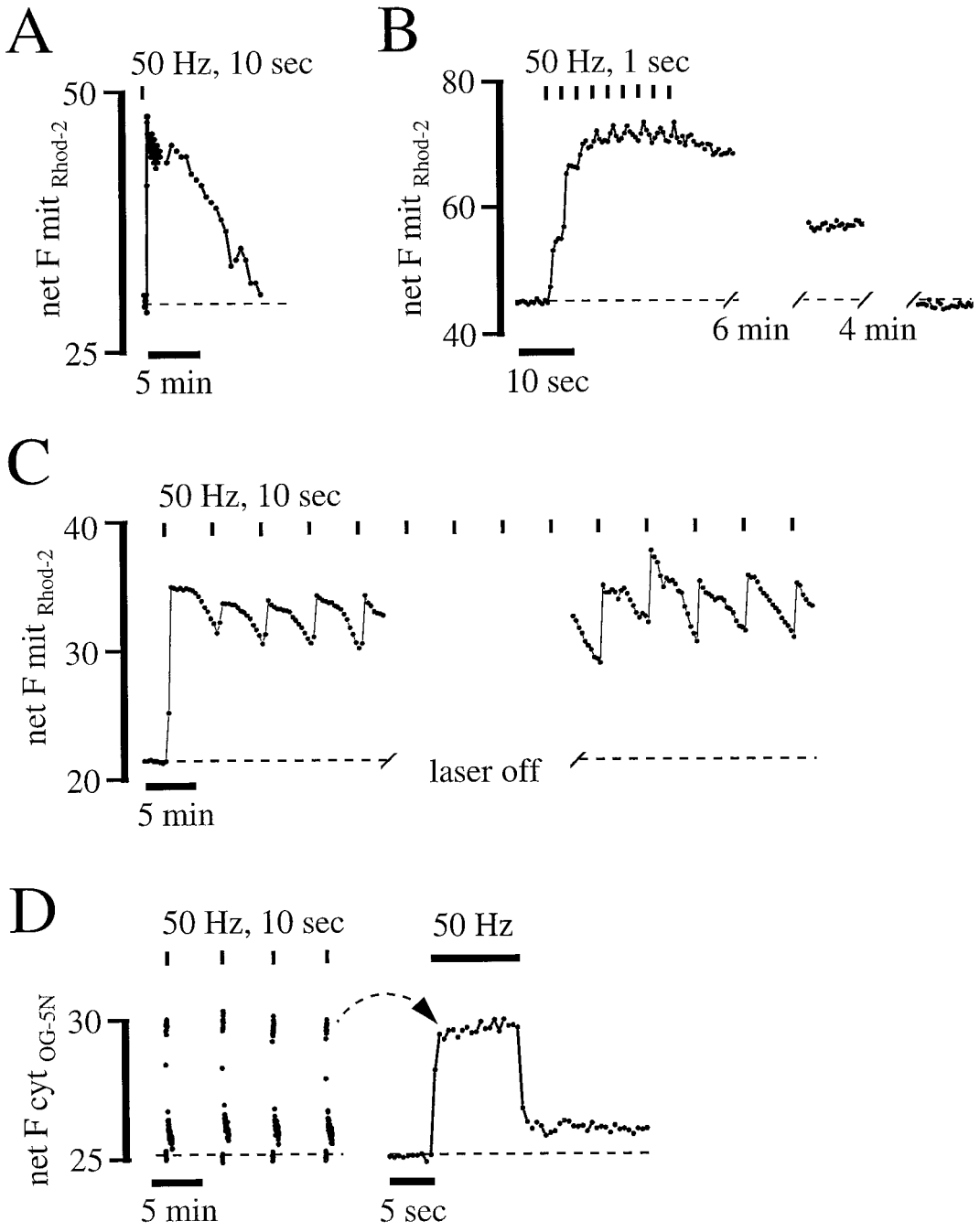

Figure 6. Changes in mitochondrial (rhod-2, *A–C*) and cytosolic (OG-5N, *D*) net fluorescence during and after steady and intermittent stimulation. *Vertical lines* above traces mark the onset of each train, not its duration. *A*, Transient evoked by 50 Hz, 10 sec train administered after a 25 min rest period. Imaging was at 2.1 sec/image for first 50 images, slowing thereafter to one image every 30 sec, to measure the prolonged decay without continuous laser illumination. *B*, Transient evoked in another terminal by nine short trains (50 Hz, 1 sec alternating with 2 sec rest intervals) preceded by a 20 min rest period. Images were sampled at 0.533 sec/image during the first 40 sec; the same imaging rate was used after the indicated 6 and 4 min periods during which the preparation was not illuminated. The fluorescence increase evoked by the second train was larger than that produced by the first, possibly because of partial saturation of matrix buffers. *C*, Transient produced by trains like that in *A* (50 Hz, 10 sec) delivered every 5 min. This was the first stimulation applied to this terminal. Fluorescence was measured at 17.066 sec/image during the first five trains. During the next ~15 min the same stimulation pattern continued without laser illumination. Laser illumination resumed for the illustrated five additional trains. *D*, Cytosolic transients in a different terminal stimulated with the same pattern as in *C* and plotted on the same time scale. This was the first stimulation applied to this terminal. The last train in the series is displayed on an expanded time scale at right. For each train, fluorescence was measured at 0.533 sec/image for 42 sec. The muscle in *B* was cleared.

stimulus train was applied to terminals that had been inactive for at least 15 min before stimulation than when the same stimulus train was applied at briefer intertrain intervals. The larger increase in mitochondrial free [Ca^{2+}] produced by the initial train was not caused by a greater elevation of cytosolic [Ca^{2+}], because the cytosolic fluorescence transient evoked by the initial train was similar to that evoked by subsequent stimulus trains (Fig. 6*D*). The increase in mitochondrial free [Ca^{2+}] produced by a given

train may depend on the initial value of mitochondrial free [Ca^{2+}], with large increases when the initial value is low (after a long rest) and smaller increases when the initial value is closer to the "ceiling" level of mitochondrial free [Ca^{2+}] measured in continuously stimulated terminals (Figs. 1, 2, 4, 6).

Changes in mitochondrial free [Ca^{2+}] during and after stimulation are consistent with reversible precipitation of a Ca salt in the mitochondrial matrix

One hypothesis to explain the stability of matrix free [Ca^{2+}] during continued mitochondrial Ca^{2+} uptake is precipitation of Ca salt(s) in the matrix. This hypothesis predicts that mitochondrial Ca^{2+} uptake will be accompanied by increases in matrix free [Ca^{2+}] during the early stages of stimulation, but that as stimulation and mitochondrial Ca^{2+} uptake continue, matrix free [Ca^{2+}] will stop increasing. Thus at these later stages matrix free [Ca^{2+}] becomes independent of total mitochondrial Ca content (Nicholls and Åkerman, 1982). Figure 7*A* diagrams such a model, and Figure 7*B*,*C* shows simulated cytosolic and mitochondrial [Ca^{2+}] transients, demonstrating that this model can account (at least qualitatively) for several features of the measured transients. For example, Figure 7*B* (*a*,*b*,*d*,*e*) shows that as stimulation frequency increases from 25 to 50 Hz, the model predicts transients similar to those measured in Figures 1*A* and 2*D*, i.e., an increase in the maximal level of cytosolic [Ca^{2+}] and in the initial rate of rise of mitochondrial [Ca^{2+}] but no increase in the maximal level of matrix free [Ca^{2+}].

During the early post-train period, mitochondria extruded Ca^{2+} into the cytosol, as evidenced by the effect of inhibiting the mitochondrial Na^+/Ca^{2+} exchanger with CGP 37157 (Fig. 5*A*). However, this initial Ca^{2+} extrusion sometimes produced little or no reduction in matrix free [Ca^{2+}] (Fig. 6*A*,*C*). The Ca salt precipitation hypothesis accounts for the delayed fall of matrix free [Ca^{2+}] after stimulation by predicting that matrix free [Ca^{2+}] will remain elevated as long as the Ca salt is dissolving and fall only after all salt has dissolved (Fig. 7*B*, *f*).

During prolonged inactivity, matrix free [Ca^{2+}] fell to low levels (Fig. 6*A*,*B*). In the model (Fig. 7*C*, *a*,*d*), as in the measurements of Figure 6*B–D*, intermittent stimulation delivered after a prolonged rest produced mitochondrial [Ca^{2+}] transients that were larger for the first few stimulus trains, although cytosolic [Ca^{2+}] transients were similar for all trains. An explanation for these findings is that total mitochondrial Ca^{2+} uptake was similar for all stimulus trains, but large increments in matrix free [Ca^{2+}] occurred only until the salt solubility product was exceeded, with further stimulus trains producing only small additional increases in matrix free [Ca^{2+}]. The model simulated the effects of mitochondrial depolarizing agents (antimycin A1 as in Fig. 2*A*,*B*; CCCP as in Fig. 4*C*,*D*) by blocking the uniporter (Fig. 7*C*, *b*,*e*).

In the simulations of Figure 7, the poorly soluble matrix salt was assumed to behave like hydroxyapatite, the least soluble Ca phosphate salt at the slightly alkaline pH (7.3–7.5) of the mitochondrial matrix. Phosphate is abundant in the mitochondrial matrix, and uptake of Ca^{2+} into isolated mitochondria is greatly increased in the presence of phosphate (Mela and Hess, 1982). In the model, the free concentration of inorganic phosphate in the matrix was assumed to be maintained by a phosphate transporter. The inner mitochondrial membrane contains a fast phosphate transporter (Ligeti et al., 1985), and total mitochondrial phosphate increases with Ca^{2+} uptake (Greenawalt et al., 1964). When Ca^{2+} uptake was simulated with only non-phosphate buffers in the matrix (Fig. 7*C*, *c*,*f*), matrix free [Ca^{2+}] rose to levels much higher than those measured, and the initial recovery of cytosolic [Ca^{2+}] was much slower. Ligeti and Lukacs (1984) found that in isolated rat liver mitochondria the presence of phosphate not only facilitated Ca^{2+} uptake but also prevented depolarization of the mitochondrial membrane potential during Ca^{2+} uptake, consistent with the absence of detectable mitochondrial depolarization during the stimulation patterns studied here (Fig. 3).

An additional argument suggests that mitochondria take up buffer (such as phosphate) during prolonged stimulation. If total matrix Ca^{2+} buffer remained constant, then one would expect that during the sustained Ca^{2+} influx associated with prolonged stimulation, the rate of change of mitochondrial free [Ca^{2+}] during stimulation would always be greater than zero. Yet measurements with both low- and high-affinity dyes showed that matrix free [Ca^{2+}] stopped increasing during prolonged stimulus trains.

Absence of phosphate transport could not be achieved experimentally. The sulfhydryl reducing agents mersalyl and *n*-ethymaleimide block phosphate transport, but their effects are not specific. Measured fluorescence transients were similar with (Fig. 2*A*) or without inorganic phosphate in the bathing solution, but it is unlikely that phosphate-free bathing solutions produced a large reduction in intraterminal phosphate because of the reservoir of phosphate in the myelinated portion of the axon.

DISCUSSION

Motor nerve terminals allow the study of changes in cytosolic and mitochondrial [Ca^{2+}] produced by controlled rates and patterns of physiological stimulation (action potential discharge) in a nondialyzed, stable preparation. The preparation permits loading of the mitochondrial matrix with either low- or high-affinity indicator dyes. Previous work demonstrated that mitochondrial [Ca^{2+}] in this preparation begins to increase after trains of only 25–50 action potentials, and that this mitochondrial Ca^{2+} uptake limits the increase in cytosolic [Ca^{2+}] during repetitive discharge (David et al., 1998). Work presented here shows that after trains of as few as 100–200 action potentials, mitochondrial free [Ca^{2+}] stops increasing, although mitochondrial uptake continues to be a major route for removing Ca^{2+} from the cytosol. After stimulation, mitochondrial free [Ca^{2+}] decays slowly (~10 min) with a complex time course.

The plateau of mitochondrial free [Ca^{2+}] during stimulation is not caused by saturation of a rapid uptake mode

Figure 7 presented a model suggesting that the plateau of matrix free [Ca^{2+}] measured during prolonged stimulation results from formation of an insoluble Ca salt within the mitochondrial matrix. Another idea that might be proffered to explain this plateau is inactivation of a "rapid uptake mode" described in isolated liver and heart mitochondria (Sparagna et al., 1995; Gunter et al., 1998). This rapid uptake mode is hypothesized to operate at cytosolic [Ca^{2+}] levels lower than those thought necessary to activate the mitochondrial uniporter, to inactivate rapidly, and to be "recharged" within a few seconds after cytosolic [Ca^{2+}] falls. However, inactivation of such a rapid uptake mode would cause cytosolic [Ca^{2+}] to keep increasing during maintained stimulation, whereas recordings showed that cytosolic [Ca^{2+}] remained stable after matrix free [Ca^{2+}] stopped increasing (Fig. 1*A*). In contrast, when mitochondrial Ca^{2+} uptake was inhibited with CCCP or antimycin A1, cytosolic [Ca^{2+}] increased throughout

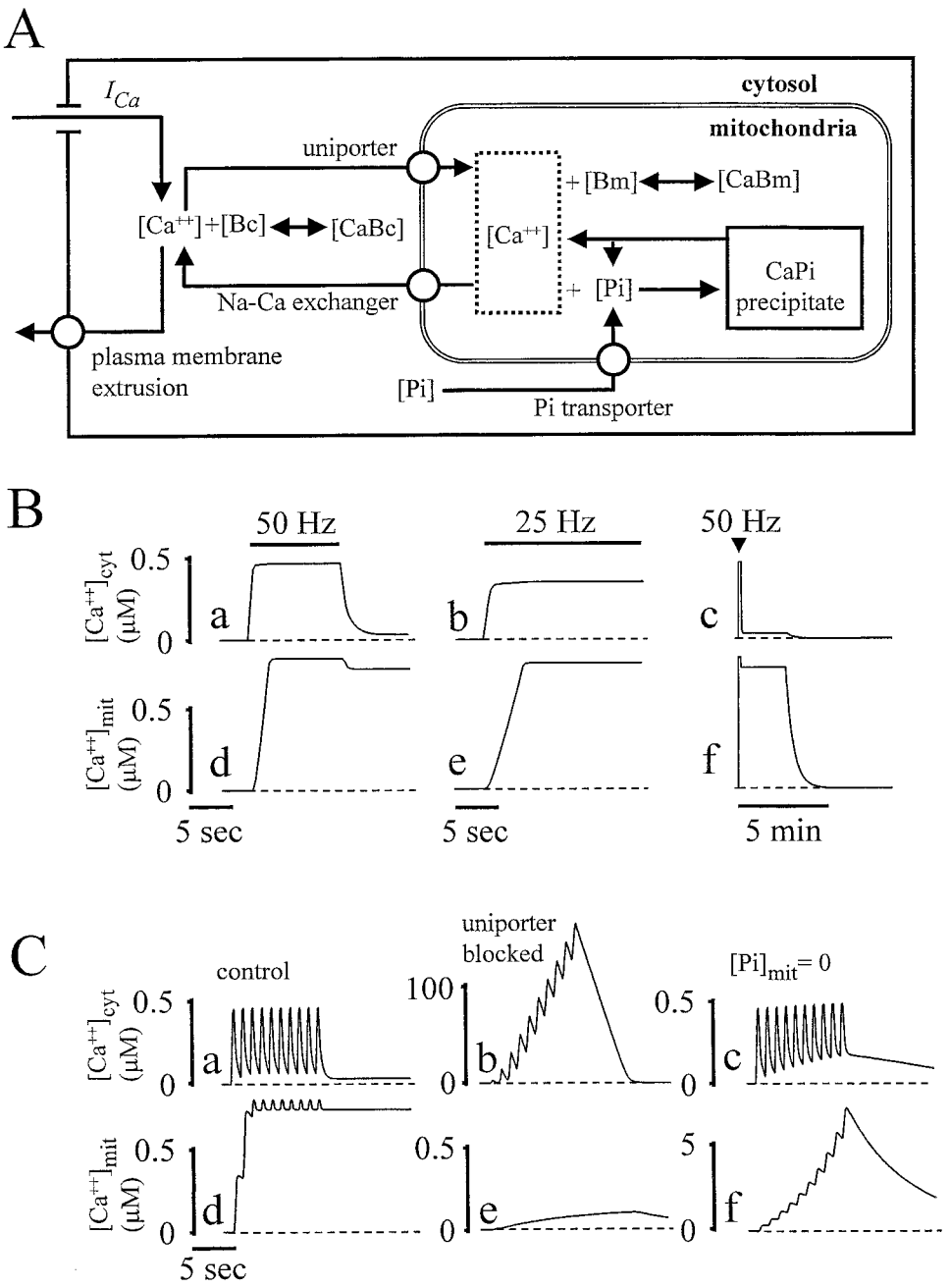

Figure 7. Simulations of stimulation-induced changes in cytosolic and mitochondrial free [Ca^{2+}] based on a model that includes reversible precipitation of a Ca phosphate salt (hydroxyapatite) in the mitochondrial matrix. *A*, Diagram of processes simulated in the model, including Ca^{2+} influx (I_{Ca}) and extrusion through the plasma membrane, Ca^{2+} uptake by the mitochondrial uniporter, Ca^{2+} extrusion via the mitochondrial Na^+/Ca^{2+} exchanger, Ca^{2+} buffering by cytosolic (*Bc*) and mitochondrial (*Bm*) buffers, and formation of a Ca-phosphate precipitate. The concentration of free mitochondrial inorganic phosphate [(*Pi*) in the form of HPO_4^{2-}] was maintained at 500 μM by a Pi transporter (except in *C*, *c*,*f*). Rates and concentrations used in the simulation are described below. *B*, Changes in cytosolic (*a–c*) and mitochondrial (*d–f*) [Ca^{2+}] during and after 50 Hz stimulation and during 25 Hz stimulation. Note the slower time scale in *c* and *f*. *C*, Changes in cytosolic (*a–c*) and mitochondrial (*d–f*) Ca^{2+} during intermittent stimulation (1 sec at 50 Hz alternating with a 2 sec rest) under control conditions (*a*, *d*), after reducing uniporter activity by a factor of 1000 (*b*, *e*) or after eliminating Pi from the mitochondrial matrix (*c*, *f*). Note the altered ordinates in *b* and *f*. Simulations were conducted using ModelMaker (Cherwell Scientific, Oxford, UK). The rate of Ca^{2+} entry across the plasma membrane during 50 Hz stimulation was 50 μM/sec [calculated from the measured increase in average cytosolic [Ca^{2+}] produced by a single action potential (20 nM; David et al., 1997) using an assumed ratio of 50 for bound/free Ca in cytosol]. Ca^{2+} extrusion across the plasma membrane, Ca^{2+} uptake via the mitochondrial uniporter, and mitochondrial extrusion of Ca^{2+} were all assumed to follow Michaelis-Menten kinetics (plasma membrane extrusion V_{max} = 10 μM/S, K_m = 0.1 μM (first order); uniporter V_{max} = 500 μM/S, K_m = 1 μM (third order dependence on cytosolic [Ca^{2+}]); mitochondrial Ca^{2+} extrusion V_{max} = 12.5 μM/S, K_m = 3 μM (first order). Total buffers and buffer K_d were 50 and 1 μM for cytosol and 5000 and 5 μM for mitochondrial matrix, respectively, with the ratio of cytosolic volume/mitochondrial volume = 10. Hydroxyapatite exhibits variable stoichiometry and complex solubility behavior; the empirical ion product [Ca^{2+}][HPO_4^{2-}] = 400 μM^2 was used to define saturation at pH >7 (Neuman and Neuman, 1958, calculated from their Fig. II-5). When this apparent solubility product was exceeded, precipitation was assumed to occur at a rate proportional to the relative supersaturation of the solution (Nancollas et al., 1989). Solvation was assumed to occur at a slow constant rate. Values for which estimates were not available in the literature were adjusted to yield plateau values of cytosolic and mitochondrial free [Ca^{2+}] similar to those measured during 50 Hz stimulation.

the stimulus train. Thus it appears that in normal saline lacking these inhibitors, mitochondrial uptake of Ca^{2+} did not inactivate or diminish during the later portions of the stimulus train. Another argument against the idea that the limited increase in mitochondrial free [Ca^{2+}] was caused by inactivation of a rapid uptake mode is that the maximal level of mitochondrial free [Ca^{2+}] did not increase when stimulus trains were separated by intervals long enough (5 min) to recharge the hypothesized rapid uptake mechanism (Fig. 6*C*).

The insoluble Ca salt hypothesis outlined in Figure 7 offers an explanation for not only the plateau of matrix free [Ca^{2+}] during prolonged stimulation, but also for other aspects of the recorded fluorescence transients such as the complex time course of decay and the dependence of transient amplitude on the intertrain interval. Many uncertainties remain concerning this model: for example, the composition of the hypothesized poorly soluble Ca salt(s), possible effects of matrix or membrane components on the solubility of these salts, the time course of their precipitation and solvation, and other possible mechanisms (besides the mitochondrial Na^+/Ca^{2+} exchanger) for removing Ca^{2+} from mitochondria. Despite these limitations, the hypothesis that much of the Ca^{2+} taken up by motor terminal mitochondria during sustained

stimulation is removed from solution in the matrix, and that this process is reversible and repeatable under physiological conditions, seems to provide the best explanation for presently available data.

Nerve terminal mitochondria accumulate Ca^{2+} at relatively low cytosolic [Ca^{2+}]

Mitochondria in motor nerve terminals begin to take up Ca^{2+} when the average cytosolic [Ca^{2+}] is ≤300 nM [stimulation-induced 200 nM increase (David et al., 1998) superimposed on an assumed resting level of ~100 nM]. Mitochondrial [Ca^{2+}] uptake at comparably low average cytosolic [Ca^{2+}] has been demonstrated in other cell types (Rizzuto et al., 1994, their Fig. 4; Babcock et al., 1997). This concentration is below the threshold [Ca^{2+}] needed to activate uniporter-mediated steady Ca^{2+} uptake in isolated liver and heart mitochondria. Various suggestions have been made to reconcile this discrepancy between measurements in isolated versus *in situ* mitochondria. One suggestion is that cytosolic factors (e.g., spermine) (Rustenbeck et al., 1993) increase the sensitivity of the mitochondrial uniporter. Another suggestion (discussed above) is that mitochondria have a rapid Ca^{2+} uptake mode, which has a higher affinity than the standard uniporter but inactivates during sustained exposure to cytosolic Ca^{2+}.

It has also been hypothesized that mitochondrial Ca^{2+} uptake occurs mainly in high [Ca^{2+}] domains within the cell, localized, for example, near IP_3-activated Ca^{2+} release channels in ER or Ca^{2+} channels in the plasma membrane (Svichar et al., 1997; Peng and Greenamyre, 1998; Csordás et al., 1999) (for review, see Rutter et al., 1998). However, several arguments suggest that stimulation-induced Ca^{2+} uptake into motor terminal mitochondria is *not* restricted to localized, high [Ca^{2+}] domains. First, synaptic vesicles (rather than mitochondria) are localized near the plasma membrane voltage-activated Ca^{2+} channels that face the synaptic cleft (Lichtman et al., 1989). Second, local Ca^{2+} domains near the plasma membrane of these motor terminals are very transient, dissipating within ~15 msec after stimulation, whereas the increase in mitochondrial [Ca^{2+}] lagged hundreds of milliseconds behind the increase in average cytosolic [Ca^{2+}] (David et al., 1997, 1998). Local domains around ER are unlikely to be important in these terminals, because drugs that deplete ER Ca^{2+} stores did not alter the maximal amplitude of the stimulation-induced increases in cytosolic and mitochondrial [Ca^{2+}] (Fig. 4*B*,*C*) (see also Tang and Zucker, 1997). Studies reporting pharmacological evidence for ER Ca^{2+} stores in motor terminals (Narita et al., 1998) used stimulation patterns much more prolonged than those applied here. Thus there is no evidence that Ca^{2+} uptake into motor terminal mitochondria during moderate stimulation required [Ca^{2+}] substantially greater than the average cytosolic values reported by indicator dyes.

Mitochondrial buffering of cytosolic Ca^{2+} may be especially prominent in synaptic terminals

Data presented here demonstrate that mitochondrial uptake is the dominant mechanism limiting the increase in cytosolic [Ca^{2+}] in lizard motor nerve terminals subjected to stimulation exceeding 25–50 action potentials at 25–100 Hz, well within the physiological range of activation of these terminals. Mitochondria appear to be similarly dominant in other synaptic terminals and in adrenal chromaffin cells (Martínez-Serrano and Satrústegui, 1992; Babcock et al., 1997; Tang and Zucker, 1997). However, there is abundant evidence for important ER contributions to handling of Ca^{2+} loads in neuronal somata (Garaschuk et al., 1997; Fierro et al., 1998). Perhaps mitochondrial Ca^{2+} uptake is especially important in cellular regions with large surface-to-volume ratios that are regularly subjected to large, rapid Ca^{2+} influxes requiring rapid sequestration. Here the ability of mitochondria to take up large amounts of Ca^{2+} by rapid passive transport might have a pronounced advantage over the slower active transport required to pump Ca^{2+} into ER stores or across the plasma membrane.

In summary, evidence presented here demonstrates that during repetitive stimulation the free [Ca^{2+}] in the mitochondrial matrix increases to up to ~1 μM, with the same maximum observed over a range of stimulation frequencies. This concentration is sufficient to activate multiple Ca^{2+}-sensitive mitochondrial dehydrogenases (for review, see McCormack et al., 1990), which are thought to help link energy production to energy demand. Mitochondria remain able to take up substantial additional Ca^{2+} after this maximal matrix free [Ca^{2+}] is attained, most likely because of import of buffer (probably phosphate) and (reversible) precipitation of Ca salts within the matrix. The hypothesized salt formation would allow mitochondria to sequester temporarily the large Ca^{2+} loads associated with stimulation of synaptic terminals while preventing excessive run-down of the mitochondrial membrane potential or elevation of intramitochondrial free [Ca^{2+}] to levels that might activate the mitochondrial permeability transition pore.

REFERENCES

Åkerman KEO, Nicholls DG (1981) Intra-synaptosomal compartmentation of calcium during depolarization-dependent calcium uptake across the plasma membrane. Biochim Biophys Acta 645:41–48.

Alnaes E, Rahamimoff R (1975) On the role of mitochondria in transmitter release from motor nerve terminals. J Physiol (Lond) 248:285–306.

Babcock DF, Hille B (1998) Mitochondrial oversight of cellular Ca^{2+} signaling. Curr Opin Neurobiol 8:398–404.

Babcock DF, Herrington J, Goodwin PC, Park YB, Hille B (1997) Mitochondrial participation in the intracellular Ca^{2+} network. J Cell Biol 136:833–844.

Baker PF, Schlaepfer W (1978) Uptake and binding of calcium by axoplasm isolated from giant axons of *Loligo* and *Myxicola*. J Physiol (Lond) 276:103–125.

Brown AC, Bullock CG, Gilmore RSC, Wallace WFM, Watt M (1985) Mitochondrial granules: are they reliable markers for heavy metal cations? J Anat 140:659–667.

Carafoli E (1987) Intracellular calcium homeostasis. Annu Rev Biochem 56:395–433.

Cox DA, Matlib MA (1993) A role for the mitochondrial Na^+-Ca^{2+} exchanger in the regulation of oxidative phosphorylation in isolated heart mitochondria. J Biol Chem 268:938–947.

Csordás G, Thomas AP, Hajnóczky G (1999) Quasi-synaptic calcium signal transmission between endoplasmic reticulum and mitochondria. EMBO J 18:96–108.

David G, Barrett JN, Barrett EF (1997) Stimulation-induced changes in [Ca^{2+}] in lizard motor nerve terminals. J Physiol (Lond) 504:83–96.

David G, Barrett JN, Barrett EF (1998) Evidence that mitochondria buffer physiological Ca^{2+} loads in lizard motor nerve terminals. J Physiol (Lond) 509:59–65.

DiLisa F, Blank PS, Colonna R, Gambassi G, Silverman HS, Stern MD, Hansford RG (1995) Mitochondrial membrane potential in single living adult rat cardiac myocytes exposed to anoxia or metabolic inhibition. J Physiol (Lond) 486:1–13.

Fierro L, DiPolo R, Llano I (1998) Intracellular calcium clearance in Purkinje cell somata from rat cerebellar slices. J Physiol (Lond) 510:499–512.

Friel DD, Tsien RW (1994) An FCCP-sensitive Ca^{2+} store in bullfrog sympathetic neurons and its participation in stimulus-evoked changes in $[Ca^{2+}]_i$. J Neurosci 14:4007–4024.

Garaschuk O, Yaari Y, Konnerth A (1997) Release and sequestration of calcium by ryanodine-sensitive stores in rat hippocampal neurones. J Physiol (Lond) 502:13–30.

Greenawalt JW, Rossi CS, Lehninger AL (1964) Effect of active accumulation of calcium and phosphate ions on the structure of rat liver mitochondria. J Cell Biol 23:21–38.

Gunter TE, Pfeiffer DR (1990) Mechanisms by which mitochondria transport calcium. Am J Physiol 258:C755–C786.

Gunter TE, Buntinas L, Sparagna GC, Gunter KK (1998) The Ca^{2+} transport mechanisms of mitochondria and Ca^{2+} uptake from physiological-type Ca^{2+} transients. Biochim Biophys Acta 1366:5–15.

Hajnóczky G, Robb-Gaspers LD, Seitz MB, Thomas AP (1995) Decoding of cytosolic calcium oscillations in the mitochondria. Cell 82:415–424.

Herrington J, Park YB, Babcock DF, Hille B (1996) Dominant role of mitochondria in clearance of large Ca^{2+} loads from rat adrenal chromaffin cells. Neuron 16:219–228.

Joó F, Párducz Á, Tóth I, Karnushina I, Barca-Barca MA (1980) Attempts at localizing calcium in relation to synaptic transmission: an X-ray microanalytical study. J Physiol (Paris) 76:403–411.

LeFurgey A, Ingram P, Lieberman M (1988) Quantitative microchemical imaging of calcium in Na-K pump inhibited heart cells. Cell Calcium 9:219–235.

Lichtman JW, Sunderland W, Wilkinson RS (1989) High resolution imaging of synaptic structure with a simple confocal microscope. New Biol 1:75–82.

Ligeti E, Lukacs GL (1984) Phosphate transport, membrane potential, and movements of calcium in rat liver mitochondria. J Bioenerg Biomembr 16:101–113.

Ligeti E, Brandolin G, Dupont Y, Vignais PV (1985) Kinetics of P_i-P_i exchange in rat liver mitochondria. Rapid filtration experiments in the millisecond time range. Biochemistry 24:4423–4428.

Magnus G, Keizer J (1997) Minimal model of β-cell mitochondrial Ca^{2+} handling. Am J Physiol 273:C717–733.

Martínez-Serrano A, Satrústegui J (1992) Regulation of cytosolic free calcium concentration by intrasynaptic mitochondria. Mol Biol Cell 3:235–248.

Matlib MA, Zhou Z, Knight S, Ahmed S, Choi KM, Krause-Bauer J, Phillips R, Altschuld R, Katsube Y, Sperelakis N, Bers DM (1998) Oxygen-bridged dinuclear ruthenium amine complex specifically inhibits its Ca^{2+} uptake into mitochondria in vitro and in situ in single cardiac myocytes. J Biol Chem 273:10223–10231.

McCormack JG, Halestra AP, Denton RM (1990) Role of calcium ions in regulation of mammalian intramitochondrial metabolism. Physiol Rev 70:391–425.

Mela L, Hess B (1982) Influence of inorganic phosphate on the kinetics of heart mitochondrial calcium accumulation. Biochem Biophys Res Commun 106:1280–1285.

Milanick MA (1990) Proton fluxes associated with the Ca pump in human red blood cells. Am J Physiol 258:C552–562.

Nancollas GH, Lore M, Perez L, Richardson C, Zawack SJ (1989) Mineral phases of calcium phosphate. Anat Rec 224:234–241.

Narita K, Akita T, Osanai M, Shirasaki T, Kijima H, Kuba K (1998) Ca^{2+}-induced Ca^{2+} release mechanism involved in asynchronous exocytosis at frog motor nerve terminals. J Gen Physiol 112:593–609.

Neuman WF, Neuman MW (1958) The chemical dynamics of bone mineral. Chicago: University of Chicago.

Nicholls D, Åkerman K (1982) Mitochondrial calcium transport. Biochim Biophys Acta 683:57–88.

Ohnuma K, Kazawa T, Ogawa S, Suzuki N, Miwa A, Kijima H (1999) Cooperative Ca^{2+} removal from presynaptic terminals of the spiny lobster neuromuscular junction. Biophys J 76:1819–1834.

Párducz Á, Jóo F (1976) Visualization of stimulated nerve endings by preferential calcium accumulation of mitochondria. J Cell Biol 69:513–517.

Park YB, Herrington J, Babcock DF, Hille B (1996) Ca^{2+} clearance mechanisms in isolated rat adrenal chromaffin cells. J Physiol (Lond) 492:329–346.

Peng TI, Greenamyre JT (1998) Privileged access to mitochondria of calcium influx through *N*-methyl-D-aspartate receptors. Mol Pharmacol 6:974–980.

Ravin R, Spira ME, Parnas H, Parnas I (1997) Simultaneous measurement of intracellular Ca^{2+} and asynchronous transmitter release from the same crayfish bouton. J Physiol (Lond) 501:251–262.

Rizzuto R, Bastianutto C, Brini M, Murgia M, Pozzan T (1994) Mitochondrial Ca^{2+} homeostasis in intact cells. J Cell Biol 126:1183–1194.

Rustenbeck I, Eggers G, Münster W, Lenzen S (1993) Effect of spermine on mitochondrial matrix calcium in relation to its enhancement of mitochondrial calcium uptake. Biochem Biophys Res Commun 194:1261–1268.

Rutter GA, Fasolato C, Rizzuto R (1998) Calcium and organelles: a two-sided story. Biochem Biophys Res Commun 253:549–557.

Sidky AO, Baimbridge KG (1997) Calcium homeostatic mechanisms operating in cultured postnatal rat hippocampal neurons following flash photolysis of nitrophenyl-EGTA. J Physiol (Lond) 504:579–590.

Somlyo AP, Somlyo AV, Shuman H, Stewart M (1979) Electron probe analysis of muscle and X-ray mapping of biological specimens with a field emission gun. Scanning Electron Micros 2:711–722.

Sparagna GC, Gunter KK, Sheu SS, Gunter TE (1995) Mitochondrial calcium uptake from physiological-type pulses of calcium. A description of the rapid uptake mode. J Biol Chem 270:27510–27515.

Stuenkel EL (1994) Regulation of intracellular calcium and calcium buffering properties of rat isolated neurohypophysial nerve endings. J Physiol (Lond) 481:251–271.

Svichar N, Kostyuk P, Verkhratsky A (1997) Mitochondria buffer Ca^{2+} entry but not intracellular Ca^{2+} release in mouse DRG neurones. NeuroReport 8:3929–3932.

Tang YG, Zucker RS (1997) Mitochondrial involvement in post-tetanic potentiation of synaptic transmission. Neuron 18:483–491.

Walrond JP, Reese TS (1985) Structure of axon terminals and active zones at synapses on lizard twitch and tonic muscle fibres. J Neurosci 5:1118–1131.

Werth JL, Thayer SA (1994) Mitochondria buffer physiological calcium loads in cultured dorsal root ganglion neurons. J Neurosci 14:348–356.

White RJ, Reynolds IJ (1995) Mitochondria and Na^+/Ca^{2+} exchange buffer glutamate-induced calcium loads in cultured cortical neurons. J Neurosci 15:1318–1328.